Simulation of Bubbly Flow in a Vertical Pipe Using Discrete Phase Model

***H.Y. Li[1], J. Lou[1], Z. Shang[1] and H. Tang[2]**

[1]Institute of High Performance Computing (IHPC), Agency for Science, Technology and Research (A*STAR), 1 Fusionopolis Way, #16-16 Connexis, Singapore 138632
[2]School of Mechanical & Aerospace Engineering, Nanyang Technology University, 50 Nanyang Avenue, Singapore 639798

*Corresponding author: lih@ihpc.a-star.edu.sg

Abstract

Bubbly flow is widely encountered in many engineering applications, such as those in chemical and nuclear systems, bubble column reactors and oil transportation pipes. Therefore, understanding of bubbly flow in a bubble-liquid flow system is extremely important. In this paper, bubbly flow involved with thousands of bubbles in a vertical pipe is numerically simulated. The motions of the bubbles are tracked using a Discrete Phase Model (DPM) and bubble-bubble interactions are simulated through the model of discrete element method (DEM). The effects of bubble diameter on the bubble flow trajectories are studied. Comparisons are made on the flow field with and without considering bubble-bubble collision.

Keywords: Bubbly flow, Discrete phase model, Bubble trajectory, DEM collision.

1. Introduction

Bubbly flow is widely encountered in many engineering applications, such as oil and gas pipes, chemical and nuclear systems (Oolman and Blanch, 1986; Chen et al., 1994) and bubble column reactors (Jakobsen, 2001). In these systems, millions of bubbles are dispersed into a continuous phase which is the carrier fluid. The movements of these bubbles have significant effects on the flow fields as well as the pressure drops in the systems. Therefore, understanding the dynamics of the bubbles is essentially important to know bubbly flow.

Experimental investigation of bubbly flow has been performed extensively (Liu and Bankoff, 1993a, 1993b; Gnotke et al., 2003; Daeseong et al., 2010). For experimental study, it generally requires large length scale test rig and high resolution measuring instruments to provide convincing data. These would lead to an extremely high cost. Meanwhile, it is rather difficult to capture the physical phenomenon occurred for each individual bubble in the experiments. In view of this, theoretical studies, in particular numerical simulations, play an essential complementary role in understanding the bubble dynamics in bubbly flow.

Bubbly flow generally involves two phases which are the carrier fluid and the bubbles. The carrier fluid is usually treated as the continuous phase in the numerical simulation. Bubbles can be treated either as a continuous phase or a discrete phase based on the methods bubbles are handled. These methods include Eulerian-Eulerian (EE) two fluid method, Lagrangian-Eulerian (LE) method and Direct Numerical Simulation (DNS) (Hirt and Nichols, 1981; Unverdi and Tryggvason, 1992; Shan, 1997; Osher and Sethian, 1988; Quan and Schmidt, 2007). EE (Drew, 1983; Enwald, 1996) two fluid model assumes bubble as another continuous phase which the average size and average velocity are chosen to represent the information for all the ranges of bubbles. Although EE model can be applied in the large scale system with both spatial and time, it is not able to represent two streams of bubbles with different velocities at the same location. The interactions among bubbles are usually not considered either. This results in the unrealistic simulations of the physical phenomena observed in the bubbly flow. Unlike EE model, LE model and DNS treat the bubbles as a discrete phase. DNS can reveal the useful detailed insights of bubble behavior and bubble interactions. Generally, it can only be applied in a system where a small number of bubbles are considered. For bubbly flow which involves thousands of bubbles, LE could be the most appropriate choice. In LE model, bubbles are represented in a Lagrangian reference frame while the carrier phase is represented in an Eulerian frame. Under such a treatment, the movement for each individual bubble in bubbly flow could be traced. The interactions among bubbles such as bubble

collision can also be included. The advantage of this method has been well documented in the paper of Subramaniam (2013).
In LE model, the trajectories of bubbles are predicted by integrating the force balance on the bubbles. The interactions between bubble and the continuous phase are achieved by the additional forces such as drag force, virtual mass force and lift force. This method has been used by Laín et al. (2002), Buwa et al. (2006), Pang et al. (2010) and Ashraf Ali and Pushpavanam (2011), to name a few, for simulation of the system with two phase flow. Zhang et al. (2005) and Xu et al. (2013) also adopted this method to investigate the dynamics of three phases including gas, liquid and particle in a multiphase system. Laín et al. (2002) evaluated the fluctuating energy existing in a bubble column system. They found that the source term in the turbulent κ-ε equations is the main issue which governs the hydrodynamic behavior of the bubbles. Buwa et al. (2006) studied the effects of geometric parameters and gas velocity on the bubble volume fraction. It is found that the recirculation flow which is observed in the experiment in the bubble columns is breakdown due to the numerical diffusion as well as the unrealistic lift force added in the simulation. Pang et al. (2010) investigated the air-water flow in a vertical channel using LE model. Their results show that most bubbles accumulated near the wall while water velocity increases at the center of the channel. Ashraf Ali and Pushpavanam (2011) compared both EE and LE model for two-phase flow in a rectangular tank. The two models agree well with each other when the gas volume fraction is low.

Bubbly flow is one of the most important flow patterns in the two phase flow in both horizontal and vertical pipes. The other flow patterns can be transited through bubbly flow by varying factors such as the bubble velocity, the bubble diameters, bubble distributions as well as the physical properties of two phases. Therefore, the effects of these parameters are extremely important for achieving a stable bubbly flow. Interesting and surprisingly, to the best knowledge of the authors, the effect of bubble diameter as well as the collision among bubbles on the flow field in the bubbly flow has not been investigated based on LE. The present work intends to fill in this gap. This paper studies air-water bubbly flow in a vertical pipe using discrete phase model which is based on LE. The flow field and bubble dynamics under different bubble diameters are investigated. In addition to this, the effect of bubble collision on the bubbly flow system is also studied.

2. Problem Description

The schematic diagram of the simulation domain is show in Fig.1(a). The radius of the cylinder *R* is 0.1m and the height is 10m. 25 air bubbles are injected into the domain at the bottom of the cylinder with a constant interval of 0.0005s. The distribution of the injected air bubble is shown in Fig. 1(b). 12 bubbles are distributed uniformly at radius of 0.07m and 0.03m, respectively. There is also another bubble located in the center of the domain. Initially, water flows into the domain with a constant speed of 1m/s. Once steady state solution of water flow is achieved, air bubbles are then injected. The injection velocity of air bubble is 0.1m/s. Driven by the buoyancy force, these air bubbles move upwardly and drive water adjacent flowing faster.

out

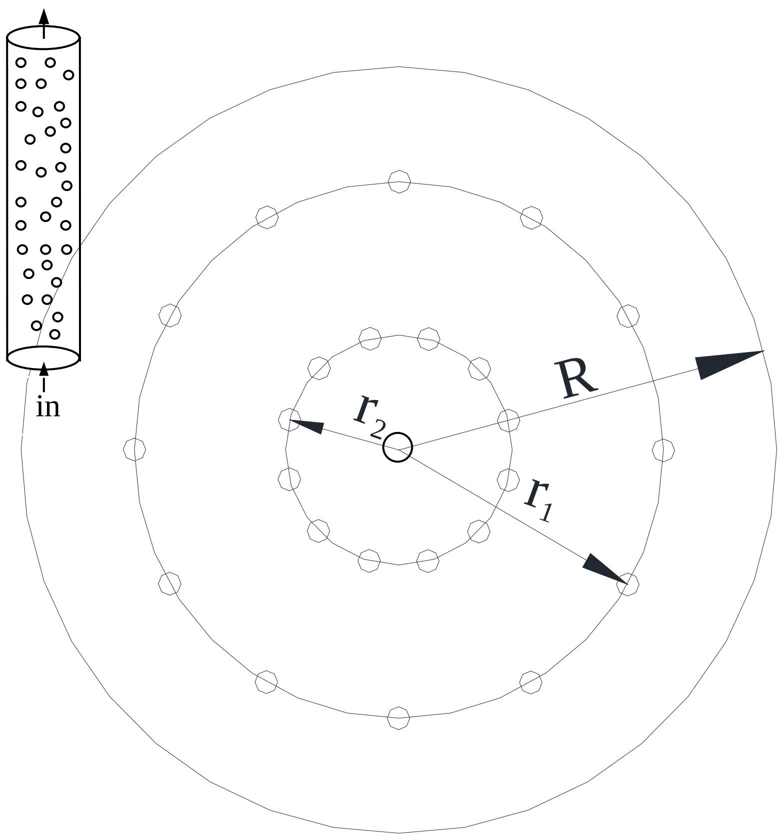

(a) (b)

Fig. 1(a) Schematic diagram of simulation domain (b) distribution of 25 injected air bubbles

3. Numerical Model

3.1 Mathematical Formulation

The trajectory of the air bubble was predicted through the integration of the force balance on the bubble based on the Lagrangian reference frame (Cundall and Strack, 1979). The mathematical formulation for bubble movement is:

$$\frac{du_{ib}}{dt} = F_D\left(u_{ib} - u_i\right) + \frac{g_i\left(\rho_b - \rho\right)}{\rho_b} + F_i \tag{1}$$

The subscript i represents the components of the axis. u_b and u are the bubble and water velocity, respectively. F_D is the drag force exerted on water by the air bubble. F_i is the other forces involved such as virtual force and pressure gradient force. As suggested by Sokolichin et al. (2004), we do not include lift force in the current work since we have no clear experimental evidence on the information of the lift force. The mathematical expression of F_D is:

$$F_D = \frac{18\mu}{\rho_b d_b^2} + \frac{C_D \,\mathrm{Re}}{24} \tag{2}$$

Where C_D is the drag force coefficient and Re is the Reynolds number. d_b is the bubble diameter. The expression for C_D and Re are, respectively:

$$C_D = a_1 + \frac{a_2}{\mathrm{Re}} + \frac{a_3}{\mathrm{Re}^2} \tag{3}$$

$$\mathrm{Re} = \frac{\rho d_b \left| u_{ib} - u \right|}{\mu} \tag{4}$$

a_1, a_2 and a_3 are constants which can be applied for spherical bubbles for all ranges of Re (Morsi and Alexander, 1972). The expressions of these constants are:

$$a_1, a_2, a_3 = \begin{cases} 0, 24, 0 & 0 < \mathrm{Re} < 0.1 \\ 3.69, 22.73, 0.0903 & 0.1 < \mathrm{Re} < 1 \\ 1.222, 29.1667, -3.8889 & 1 < \mathrm{Re} < 10 \\ 0.6167, 46.50, -116.67 & 10 < \mathrm{Re} < 100 \\ 0.3644, 98.33, -2778 & 100 < \mathrm{Re} < 1000 \\ 0.357, 148.62, -47500 & 1000 < \mathrm{Re} < 5000 \\ 0.46, -490.546, 578700 & 5000 < \mathrm{Re} < 10000 \\ 0.5191, -1662.5, 5416700 & \mathrm{Re} \geq 10000 \end{cases} \tag{5}$$

$$F_i = 0.5 \frac{\rho}{\rho_b} \frac{d\left(u_i - u_{ib}\right)}{dt} + \frac{\rho}{\rho_b} u_{ib} \frac{\partial u_{ib}}{\partial x_i} \tag{6}$$

The bubbles are carried by a flowing fluid. To model the continuous phase flow, the incompressible forms of the continuity and the Navier-Stokes with considering turbulent flow equations are employed for the simulation domain.

$$\frac{\partial \rho}{\partial t} = \frac{\partial}{\partial x_i}\left(\rho u_i\right) \tag{7}$$

$$\frac{\partial}{\partial t}\left(\rho u_i\right) + \frac{\partial}{\partial x_j}\left(\rho u_i u_j\right) = -\frac{\partial p}{\partial x_i} + \frac{\partial}{\partial x_j}\left[\mu\left(\frac{\partial u_i}{\partial x_j} + \frac{\partial u_j}{\partial x_i}\right) - \frac{2}{3}\delta_{ij}\rho\kappa\right] + \frac{\partial}{\partial x_j}\left(-\rho \overline{u_i' u_j'}\right) \tag{8}$$

The turbulent flow is simulated through κ-ε model which is embedded in FLUENT.

3.2 Geometry Mesh

The geometry of the simulation domain is meshed using GAMBIT 2.4. A uniform mesh size of 5 mm and a total of 2.8 million cells are used for the whole domain. Such mesh is chosen based on the grid independency study among the mesh cells of 1.8 million, 2.8 million and 4.2 million.

3.3 Boundary conditions

The current simulation is performed using ANSYS FLUENT 14. Initially, water single-phase flow under steady state simulation is carried out. Once the steady state solution of water flow is achieved, air bubbles are then injected into the domain. Bubbles are tracked in a transient basis with a time step size of 0.0005s. The inlet velocity of water is 1m/s and the inlet velocity of bubble is 0.1m/s. An atmosphere pressure is set at the outlet boundary. No slip boundaries are applied on the walls for water. For air bubbles on the walls, reflection with no energy loss is assumed.

4. Results and Discussion

4.1 Validation

The current numerical simulation is validated with the experimental work done by Ohnuki and Akimoto (2000). Figure 2 shows the comparison of pressure drop under different air inlet velocity. The inlet water velocity is fixed at 1.06m/s. Generally, the increase of air velocity increases its volume fraction. This leads to a low pressure drop in a vertical pipe. Good agreement was achieved between the experimental data and simulation results.

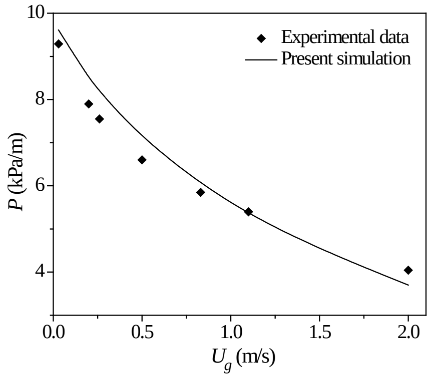

Fig. 2 Comparison of pressure drop under different air velocity

4.2 Air bubble and water velocity without considering bubble collision

Figure 3(a) and 3(b) show the bubble and water velocity at different locations, respectively. As the bubbles are tracked in a transient basis, bubble velocity is shown at different times. Figure 3(a) shows the bubble velocity at t = 2s at r = 0, 0.03m and 0.07m. r = 0 is the center of the pipe. The diameter of bubbles introduced into the pipe is 300μm. A significant increase of bubble velocity is observed as seen from Fig. 3(a) in a short time once bubbles are injected into the domain. This is due to the dominance of buoyancy force at the initial stage in the bubble rising process. Such velocity increases to its maximum value of 3.2m/s at around t = 0.05s and after that, bubble velocity decreases. The increase of bubble velocity increases the drag force between bubble and water. When the drag force becomes dominated, bubble velocity starts to decrease. Similar trends have been found for the bubble velocity at different locations before t = 0.1s. This is not what observed thereafter. After t = 0.1s, a slightly increase of bubble velocity is found for the bubbles at the center of the domain while a further decrease of bubble velocity is seen at r = 0.03 and 0.07m. Water velocity at t = 2s is shown in Fig. 3(b). Compared with water single phase flow at different locations, water velocity with air bubble inside shows significantly difference from its corresponding partner before 4.5 m along the height of the pipe. The length of 4.5m actually is the travel distance for the air bubbles in the duration of 2s. With air bubbles injected into the domain, these bubbles rise quickly given the buoyancy force. They exert high drag force to water and drive water surrounding moving faster. Therefore, water velocity increases. However, the injection of air bubbles in water enhances the instability of the flow field. As a consequence, water velocity exemplifies fluctuated styles which reveal the random and chaotic flow behavior once bubbles are introduced. Water velocity is higher than its counterpart at r = 0 while at the other two locations, water velocity is lower than its counterpart after the length of 1m. Unlike velocity in the length of 4.5m, water velocity is less affected by air bubble in the pipe length where air bubble has not reached. Those lines are overlapped together with its counterpart at different locations upon achieving to the end of the pipe.

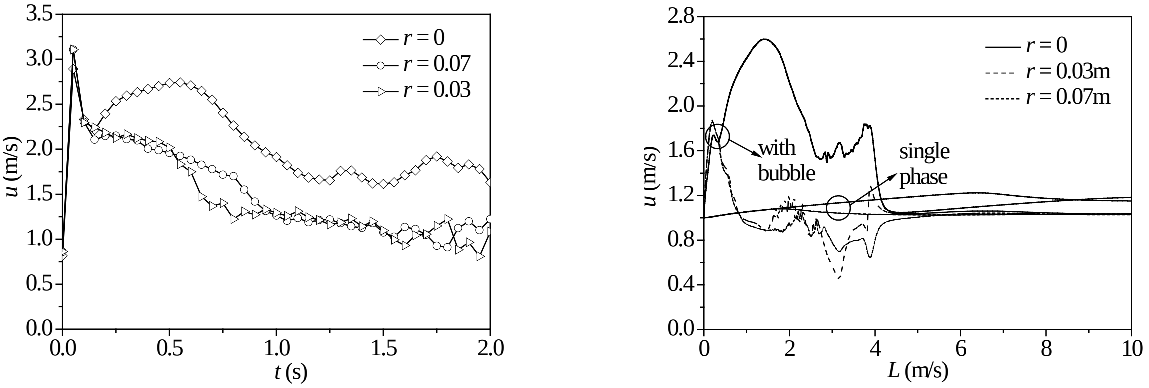

(a) (b)

Fig. 3 Variations of (a) particle velocity under different times, (b) water velocity along the pipe at t = 2s

Figure 4(a) and 4(b) show air bubble and water velocity at different radial locations at t = 4.5s, respectively. Fluctuations of the air bubble velocity is seen after t = 3.0s. Bubble flow in water actually increases the intensity of turbulent flow which leads to the fluctuation of both water and air bubble velocity. Such fluctuation is generally irregular and chaotic. A dramatic fluctuation in water velocity is initially observed at the center of the pipe and then it propagates to other locations. The travel distance for bubbles at t = 4.5s is around 9m which is indicated by the variation of water velocity in Fig. 4(b).

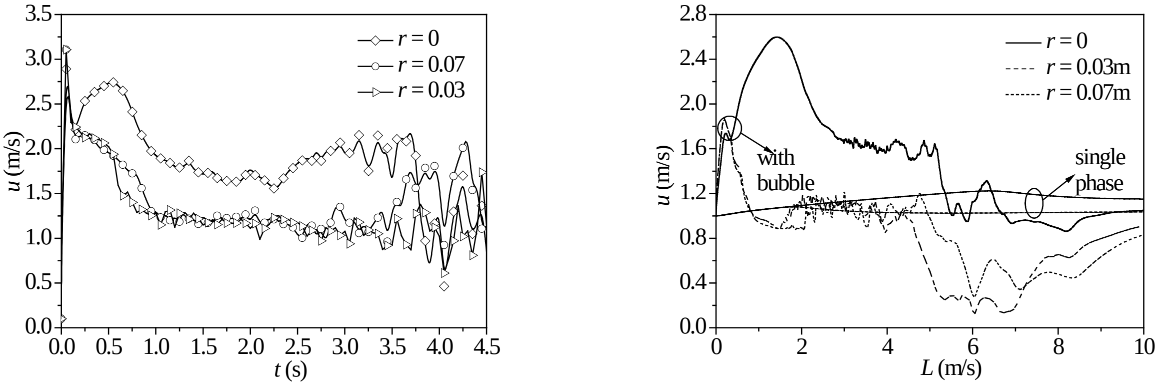

(a) (b)

Fig. 4 Variations of (a) particle velocity under different times, (b) water velocity along the pipe at t = 4.5s

Figure 5(a) and 5(b) show air bubble and water velocity at t = 10s at different locations, respectively. At this time, the number of bubbles entering and escaping from the pipe is almost equivalent. The number of bubble reside in the pipe is around 36 thousand. The flow field become much more chaos as can be seen from the fluctuation of both water and air bubble velocity. Generally, air bubble and water velocity at the center of the pipe is larger than those at other radial locations. This is not the situation when fluctuations occur. The existence of bubble changes the flow dynamic significantly.

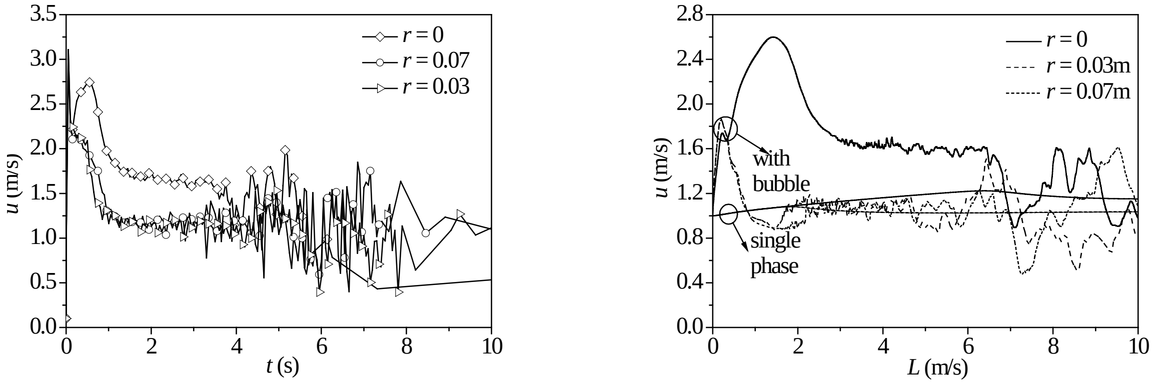

(a) (b)

Fig. 5 Variations of (a) particle velocity under different times, (b) water velocity along the pipe at *t* = 10s

The effect of bubble diameter on water flow velocity at *r* = 0 is shown in Fig. 6. Such water velocity is chosen when the number of bubble entering and escaping from the pipe is the same. It is surprised to find water velocity with considering bubbles is the same as that without considering bubbles when the bubble diameter is 3μm. This implicates there is a critical bubble diameter under which the flow filed acts as no bubbles involved. For the case where the bubble diameter is above the critical value, there is no much difference on the water velocity along the length of 2.5m of the pipe under different bubble diameters. Thereafter, water velocity fluctuates. Generally, the larger the bubble diameter, the higher the fluctuation is.

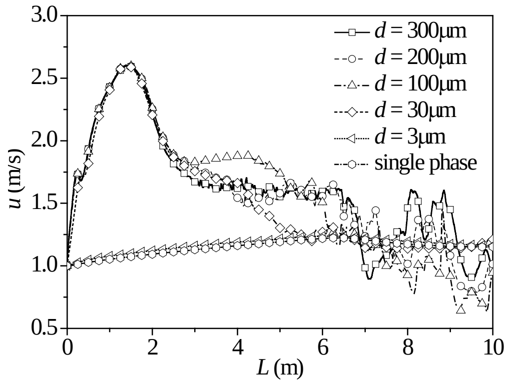

Fig. 6 Effect of bubble diameter on water velocity at *r* = 0

4.3 The effect of bubble collision on the air bubble and water velocity

Bubble collision is simulated based on the spring collision law where no energy loss is considered. Bubble and water velocity at *r* = 0.07m with and without considering collision model under different bubble diameters is shown in Fig. 7(a) and 7(b), respectively. For bubble diameter of 3μm, the inclusion of the bubble collision has no effects on both the bubble and water velocity. This is not the case for bubble diameter of 300μm. For bubble diameter of 300μm, bubble collision is not significant at initial time as both bubble and water velocity are overlapped together first. Since then, large differences are found. The inclusion of bubble collision enhances the chaotic of the bubble dynamics. Therefore, a large fluctuation of bubble velocity is expected as seen from Fig. 7(a) after *t* = 3s. The large fluctuation of bubble increases the fluctuations of the water velocity simultaneously.

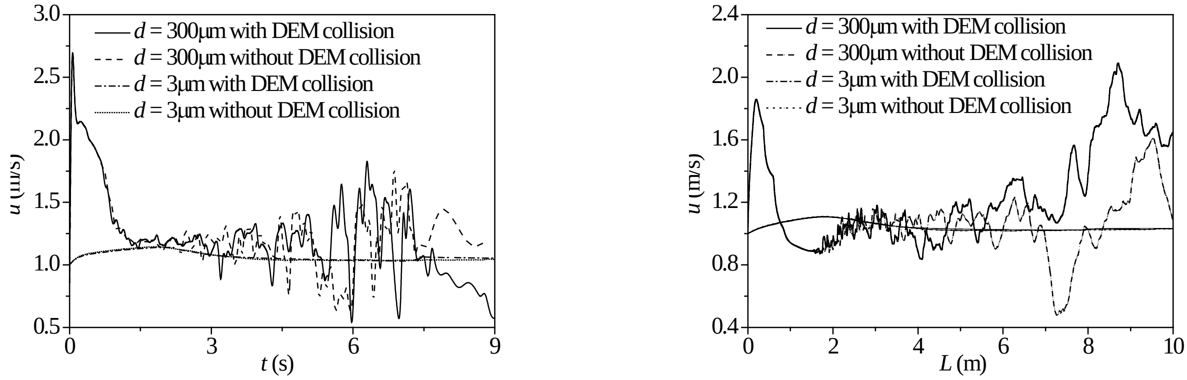

(a) (b)

Fig. 7 Comparison of (a) bubble, and (b) water velocity with and without bubble collision at r = 0.07m

Drag force is another important force in the bubbly flow. The comparison of drag force coefficient along the pipe with and without considering bubble collision is shown in Fig. 8. Given the fluctuation of the bubble and water velocity, the drag coefficient also shows a fluctuated mode. A higher fluctuation is observed with considering bubble collision compared with that without considering bubble collision.

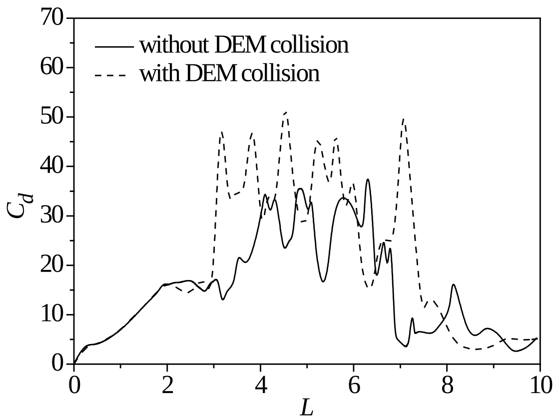

Fig. 8 Comparison of drag coefficient for d = 300μm

5. Conclusions

In this paper, bubbly flow is simulated through DPM based on LE model. The effect of bubble diameter as well as bubble collision on the flow field is investigated. It is found that the involvement of the bubbles forces the flow field fluctuated. A high fluctuation is observed under large bubble diameter. However, when the bubble diameter is sufficiently small, the dynamic of bubble in the flow filed has no effect on the fluid flow even bubble collision is considered. The inclusion of the bubble collision enhances the fluctuation of the flow filed as well.

References

Ashraf Ali, B. and Pushpavanam, S. (2011), Analysis of unsteady gas-liquid flows in a rectangular tank:comparison of Euler-Eulerian and Euler-Lagrange simulations. *International Journal of Multiphase Flow*, 37, pp. 268-277.

Buwa, V.V., Deo, D.S. and Ranade, V.V. (2006), Eulerian-Lagrangian simulations of unsteady gas-liquid flows in bubble columns, *International Journal of Multiphase Flow*, 32, pp. 864-885.

Chen, R.C., Reese, J. and Fan, L.S. (1994), Flow structure in three-dimensional bubble column and three-phase fluidized bed. *AIChE Journal*, 42, pp. 1093-1104.

Cundall P.A. and Strack O.D.L. (1979), A discrete numerical model for granular assemblies. *Géotechnique*, 29, pp. 47-65

Daeseong, J., Shripad, T. and Revankar, T. (2010), Effect of coalescence and breakup on bubble size distributions in a two-dimensional packed bed. *Chemical Engineering Science*, 65, pp. 4231-4238.

Drew, D**.** A**.** (1983), Mathematical modeling of two-phase flow**.** *Annual Review of Fluid Mechanics*, 15, pp. 261-291.

Enwald, H., Peirano,E., Amstedt A.E.(1996), Eulerian two-phase flow theory applied to fluidization. *International Journal of Multiphase Flow*, 22, pp.21-66.

Gnotke, O., Benk, H. and Loth, R. (2003), Experimental study on the number density distribution function in turbulent bubbly flows with coalescence and break-up. *Experimental Thermal and Fluid Science*, 27, pp. 803–816.

Hirt, C. W. and Nichols, B. D. (1981), Volume of fluid /VOF/ method for the dynamics of free boundaries. *Journal of Computational Physics*, 39, pp. 201-225.

Jakobsen, H.A. (2001), Phase distribution phenomena in two-phase bubble column reactors. *Chemical Engineering Science*, 56, pp.1049-1051.

Laín, S., Bröder, D., Sommerfeld,M. and Göz,M.F. (2002), Modeling hydrodynamics and turbulence in a bubble column using the Euler-Lagrange procedure. *International Journal of Multiphase Flow*, 28, pp. 1381-1407.

Liu, T.J. and Bankoff, S.G. (1993a), Structure of air-water bubbly flow in a vertical piple, I. liquid mean velocity and turbulence measurement. *International Journal of Heat and Mass Transfer*, 36, pp. 1049-1060.

Liu, T.J. and Bankoff, S.G. (1993b), Structure of air-water bubbly flow in a vertical piple, II.void fraction, bubble velocity and bubble size distribution. *International Journal of Heat and Mass Transfer*, 36, pp. 1061-1072.

Moris, S.A. and Alexander, A.J. (1972), An investigation of particle trajectories in two-phase flow systems. *Journal of Fluid mechanics*, 55, pp. 193-208.

Ohnuki, A. and Akimoto, H. (2000), Experimental study on transition of flow pattern and phase distribution in up-ward air-water two-phase flow along a large vertical pipe. *International Journal of Multiphase Flow*, 26, pp. 367-386.

Oolman, T. and Blanch, H.W. (1986), Bubble coalescence in air-sparged bioreactor. *Biotechnology and Bioengineering*, 28, pp. 578-584.

Osher, S. and Sethian, J.A. (1988), Fronts Propagating with Curvature-Dependent Speed: Algorithms Based on Hamilton-Jacobi Formulations. *Journal of Computational Physics*, 79, pp. 12-49.

Pang, M.J., Wei, J.J. and Yu, B. (2010), Numerical study of bubbly upflows in a vertical channel using the Euler-Lagrange two-way model. *Chemical Engineering Science*, 65, pp. 6215-6228.

Quan, S.P. and Schmidt, D.P. (2007), A moving mesh interface tracking method for 3D incompressible two-phase flows. *Journal of Computational Physics*, 221, pp. 761-780.

Shan, X. (1997), Simulation of Rayleigh-Bénard convection using a Lattice Boltzmann Method. *Physical Review E*, 55, pp. 2780-2788.

Sokolichin, A., Eigenberger, G. and Lapin, A. (2004), Simulation of buoyancy driven bubbly flow:established simplifications and open questions. *Fluid Mechanics and Transport Phenomena*, 50, pp. 24-45.

Subramaniam, S. (2013), Lagrangian Eulerian methods for multiphase flows. *Progress in Energy and Combustion Science*, 39, pp. 215-245.

Unverdi, S. O. and Tryggvason, G. (1992), A front-tracking method for viscous, incompressible, multi-fluid flows. *Journal of Computational Physics*, 100, pp. 25-37.

Xu, Y.G., Liu, M.Y. and Tang,C. (2013), Three-dimensional CFD-VOF-DPM simulations of effects of low-holdup particles on single-nozzle bubbling behavior in gas-liquid-solid system. *Chemical Engineering Journal*, 222, pp. 292-306.

Zhang X., Ahmadi, G. (2005), Eulerial_lagrangian simulations of liquid-gas-solid flows in three-phase slurry reactors, *Chemical Engineering Science*, 60, pp. 5089-5104.